

# Electronic structure of $\text{HgBa}_2\text{CuO}_{4+\delta}$ with self-organized interstitial oxygen wires in the Hg spacer planes

Thomas Jarlborg<sup>1,2</sup> and Antonio Bianconi<sup>2,3,4</sup>

<sup>1</sup> DPMC, University of Geneva, 24 Quai Ernest-Ansermet, CH-1211 Geneva 4, Switzerland

<sup>2</sup> RICMASS Rome International Center for Materials Science Superstripes, Via dei Sabelli 119A, 00185 Rome, Italy

<sup>3</sup> Institute of Crystallography, Consiglio Nazionale delle Ricerche, CNR, Via Salaria Km 29.300, Monterotondo, Roma, I-00015, Italy

<sup>4</sup> National Research Nuclear University MEPhI (Moscow Engineering Physics Institute), Kashirskoe sh. 31, 115409 Moscow, Russia

While recent experiments have found that at optimum doping for the highest critical temperature in  $\text{HgBa}_2\text{CuO}_{4+y}$  ( $\text{Hg1201}$ ) the oxygen interstitials (O-i) are not homogeneously distributed but form one-dimensional atomic wires, there are no available information of its electronic structure considering self-organized O-i atomic wires. Here we report the calculated electronic structure of  $\text{HgBa}_2\text{CuO}_{4+y}$  where oxygen interstitials form atomic wires along (1,0,0) crystal direction in the Hg layer. We find that at optimum doping for superconductivity the chemical potential is tuned near an electronic topological Lifshitz transition for the appearing of a second quasi 1D Fermi surface. A *first* large Fermi surface coexists with a *second* incipient quasi one dimensional (1D) Fermi surface related with atomic wires of oxygen interstitials. Increasing oxygen doping the chemical potential is driven to the band edge of the *second* 1D-band giving a peak in the density-of-states. The new 1D electronic states are confined near the oxygen interstitial wires with a small spread only on nearby sites. Spin-polarized calculations show that the magnetic response is confined in the oxygen-poor domains free of oxygen interstitials wires and it is quite insensitive to the density of O-i wires.

PACS numbers: 74.20.Pq, 74.72.-h, 74.25.Jb

## I. INTRODUCTION.

In these last years novel experiments have observed that the self-organization of interstitials and defects can dramatically enhance or suppress the critical temperature  $T_c$  in cuprates [1–3]. The self-organization of defects and interstitials in the spacer layers depends on the lattice misfit *strain* between the spacer layers and the  $\text{CuO}_2$  layers. The lattice strain has been proposed to be the third axis of the 3D phase diagram  $T_c$ , *doping*, *strain* for all cuprates families [4]. In  $\text{Bi}_2\text{Sr}_2\text{CaCu}_2\text{O}_{8+y}$  ( $\text{Bi2212}$ ) the misfit strain induces a relevant corrugation of the  $\text{CuO}_2$  planes observed by Cu K-edge Resonant Elastic X-ray Scattering (REXS) [5] accompanied by the superconducting gap modulation [6, 7]. The formation of stripes in cuprates has been first observed using synchrotron radiation x-ray spectroscopy which probes the local structure in  $\text{Bi}_2\text{Sr}_2\text{Ca}_{1-x}\text{Y}_x\text{Cu}_2\text{O}_{8+y}$  [8–11] due to cooperative effects of misfit strain and CDW formation with wave-vector depending on doping [12, 13]. The investigation of the variation of the critical temperature in complex defective transition metal oxides as a function of interstitials organization has provided evidence for defects and interstitials organization in  $\text{Na}_x\text{CoO}_2+y\text{D}_2\text{O}$  ( $x=1/3$ ;  $y=4x$ ) [14] and in  $\text{Sr}_3\text{Co}_2\text{O}_x$  ( $5.64 < x < 6.60$ ) [15]. The defects self organization controlling the critical temperature has been found in  $\text{Sr}_2\text{CuO}_{4-y}$  [16], in  $\text{Sr}_{2-x}\text{Ba}_x\text{CuO}_{3+y}$  [17], in  $(\text{Cu}_{0.75}\text{Mo}_{0.25}\text{Sr}_2\text{YCu}_2\text{O}_{7+y})$  with  $0 < y < 0.5$  [18, 19], and in  $\text{BaPb}_{1-x}\text{Bi}_x\text{O}_3$  [20]. The oxygen interstitial organization in oxygen doped cuprates  $\text{La}_2\text{CuO}_{4+y}$  has been studied by scanning micro x-ray diffraction [2, 3, 21–26], and by STM [27–29]

showing superconductivity emerging in a nanoscale phase separation with a complex geometry [30–34]. The phase separation is determined by the proximity to a electronic topological Lifshitz transition in strongly correlated electronic systems [35–37]. There is now growing agreement that the domes of high critical temperature in different superconductors occur where the chemical potential is tuned near topological electronic Lifshitz transitions [38–42] including the case of pressurized sulfur hydride [43–45].

A considerable theoretical work has shown how the electronic states near the Fermi level respond to the lattice and dopants organization changing the topology of the Fermi surface [46–53]. The interest is driven by the perspective that a the quasi one-dimensional ordering of dopants could generate stripes giving a new incipient quasi 1D electronic structure at the Fermi level which is expected to enhance the critical temperature. The stripes periodicity driven by oxygen interstitial self organization sets up a potential modulation, where the chemical potential is tuned at a Lifshitz transition for the appearing of a new 1D band. The lattice structure of the stripes and the charge density have to be tuned so that one of the peaks of the density of states is near the position of the chemical potential. Doping is crucial for high- $T_c$  superconductivity. It can be controlled either by the substitution of the heavy atoms with different valency, like Sr (or Ba) for La in  $\text{La}_{2-x}\text{Sr}_x\text{CuO}_4$ . or by varying the oxygen content which has been proven to be efficient for doping, either as a vacancy or as an interstitial impurity. Superconductivity can be enhanced by ordering of oxygen interstitials in cuprates like  $\text{La}_2\text{CuO}_{4\pm\delta}$  [3]. Band

calculations show that oxygen vacancies in the apical positions in  $\text{Ba}_2\text{CuO}_{4-\delta}$  (BCO, with  $\delta \approx 1$ ) make its electronic structure very similar to that of optimally doped  $\text{La}_2\text{CuO}_4$  (LCO) [49, 50]. The  $T_c$  of BCO is reported to be much larger than in LCO [17]. Self organization of oxygen interstitials enhances  $T_c$  [3], and the Fermi surface (FS) can become fragmented by oxygen self organization [47]. However, the exact role of *ordering* of the defects is not well known in many cases.

Recently experimental results have been reported on self organization of oxygen interstitials in doped cuprates  $\text{HgBa}_2\text{CuO}_{4+y}$  [54, 55]. by scanning micro x-ray diffraction which provide complementary information on local nanoscale structure investigation using x-ray absorption spectroscopy [56–58] using EXAFS and XANES methods [59, 60] which probe the deviation of the local structure from the average structure. In this work we present electronic structure results for the hole-doped oxygen-enriched  $\text{HgBa}_2\text{CuO}_{4.167}$ . Ordered O-stripes with 2 impurities along (0,1,0) are separated by 5 unit cells along (1,0,0). Cells with disordered distribution of the two O impurities and without impurities are studied for comparison. The method of calculation is presented in sect. II. Experimental information about the structure is used to define the supercells of O-rich LNO, as is also discussed in sect. II. In sect. III we discuss the results of the calculations, and some ideas for future works are given together with the conclusions in sect. IV.

## II. METHOD OF CALCULATION.

The calculations are made using the linear muffin-tin orbital (LMTO) method [61, 62] and the local spin-density approximation (LSDA) [63, 64]. The details of the methods have been published earlier [47, 53, 65, 66]. The supercell  $\text{Hg}_{12}\text{Ba}_{24}\text{Cu}_{12}\text{O}_{48+2}$  is extended 6- and 2-lattice constants along  $x$  and  $y$ , respectively. The 2 additional oxygens are inserted in the Hg-plane, as is known to be the position of excess O in HBCO. These oxygen interstitials form a stripe running along  $y$ . Calculations for the elementary cell of HBCO need 8 atomic sites and 5 "empty spheres", which are included in the most open part of the structure, see ref. [65]. The empty sphere in the Hg plane, at (0.5, 0.5, 0), is the location of excess oxygen. The lattice constant  $a_0=3.87$  Å, and  $c/a=2.445$ . The elementary cell is extended  $6a_0$  along  $x$  and  $2a_0$  along  $y$ . The empty spheres at (0.5, 0.5, 0) and (0.5, 1.5, 0), and at (0.5, 0.5, 0) and (2.5, 1.5, 0) are occupied by O in the "stripe" supercell and "disordered" supercells, respectively. This is in the latter case the most distant and uncorrelated choice for the two interstitial O impurities. The band calculations are made for this supercell containing 156 sites totally, and the basis set goes up through  $\ell=2$  for atoms and  $\ell=1$  for empty spheres. Self-consistent, paramagnetic and spin-polarized calculations are made for these cells using 54 k-points. The FS plots used a finer k-point mesh, 210 k-points, in one plane

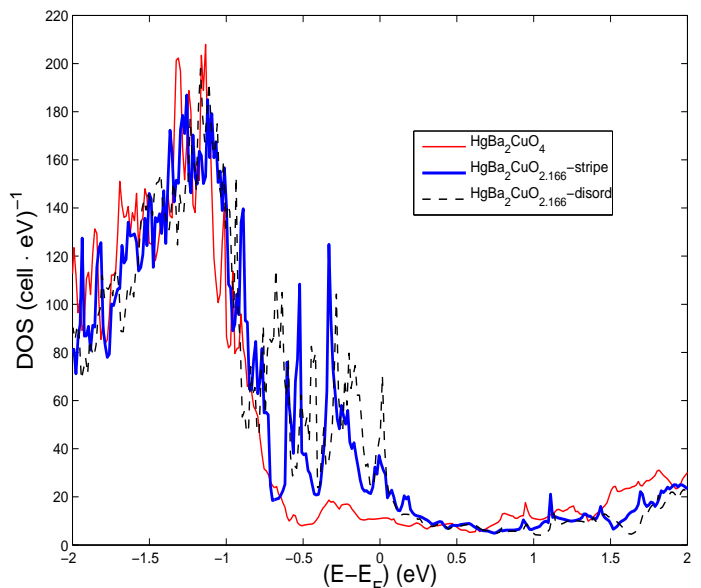


FIG. 1: (Color online) The total DOS for  $\text{Hg}_{12}\text{Ba}_{24}\text{Cu}_{12}\text{O}_{48+N}$  with  $N=0$  (thin red) and  $N=2$  (bold blue). The (black) broken line is when the 2 O atoms occupy sites far from each other ("disordered").

half-way of the maximum  $k_z$ .

Correlation is not expected to be an issue for cuprates and nickelates with doping well away from half-filling of the d-band. This is confirmed for cuprates from ARPES (angular-resolved photoemission spectroscopy) and ACAR (angular correlation of positron annihilation radiation), which detect FS's and bands that evolves with high doping in agreement with DFT (density-functional theory) calculations [67–69].

TABLE I: Local decomposition of the DOS at  $E_F$  (in units of  $(\text{atom} \cdot \text{eV})^{-1}$ ) for  $\text{Hg}_{12}\text{Ba}_{24}\text{Cu}_{12}\text{O}_{48}$  and "striped" and "disordered"  $\text{Hg}_{12}\text{Ba}_{24}\text{Cu}_{12}\text{O}_{48+2}$ . The total  $N(E_F)$  are 11.0, 37.0 and 47.5  $(\text{cell} \cdot \text{eV})^{-1}$ , respectively. Apical and planar O are indicated  $\text{O}_{ap}$  and  $\text{O}_{pl}$ , respectively. The additional impurity oxygens ( $\text{O}_i$ ) have very large p-DOS, but also all atoms in the first layer around an impurity get large DOS values.

		Ba	Hg	Cu	$\text{O}_{ap}$	$\text{O}_{pl}$	$\text{O}_i$
undoped		-	-	0.73	-	0.12	
stripe	near $\text{O}_i$	0.02	0.84	1.0	0.50	0.21	5.5
	far from $\text{O}_i$	-	-	0.93	0.15	0.18	
disord.	near $\text{O}_i$	0.3	0.46	1.1	0.29	0.20	8.0
	far from $\text{O}_i$	-	-	0.90	0.03	0.15	

## III. RESULTS AND DISCUSSION.

The nonmagnetic (NM) total DOS functions at the Fermi level for the three supercells are shown in Figs.

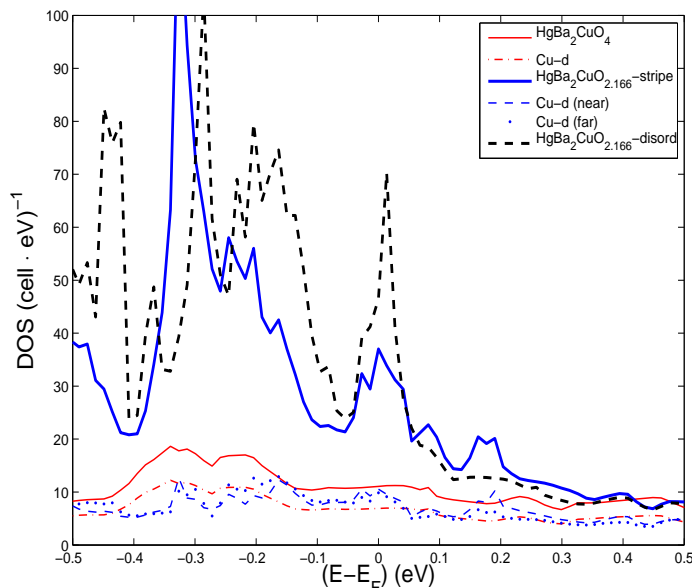


FIG. 2: (Color online) The DOS functions in Fig. 1 on a finer energy scale. The partial Cu-d DOS are also shown for the undoped case (red semi-broken) and the striped case for Cu near to (blue dotted) and far from (blue thin broken) the  $O_i$ -stripe. The partial Cu-d DOS function are multiplied by 12 in order to be normalized to the total DOS.

1. The undoped DOS agree with the DOS calculated previously for one unit cell of HBCO using also  $\ell = 3$  states for the Ba sites [65]. A difference is that the less dense k-point mesh for the supercell makes the DOS curve less smooth. The total DOS at  $E_F$  per elementary cell is about  $1.0 \text{ (eV)}^{-1}$  compared to  $0.92$  here for the supercell. A calculation of a supercell of intermediate size ( $\text{Hg}_4\text{Ba}_8\text{Cu}_4\text{O}_{17}$ ) corresponding to an impurity concentration of  $0.25$  shows that the DOS at  $E_F$  increases by a factor of two to about  $1.8$  per elementary cell [52]. All atoms are close to the impurity in that case, which explains that the local peaks in the states are not so narrow as in the present case. Here  $E_F$  is on a narrow peak in both cells with O impurities, which makes the DOS higher, about  $3$  and  $4 \text{ (eV)}^{-1}$  per elementary cell for the striped and disordered case respectively. The increase of the DOS is limited to the first layers of atoms adjacent to the impurity, see Table I. Hybridization with the p-states on the oxygen impurity atoms makes large s- and d-DOS on Hg, and large increase of the p-DOS on apical oxygen states, while the changes on planar O and Ba are not large. The Cu sites are quite distant to the  $O_i$ . Nevertheless, the Cu d-DOS goes up by about 35 percent near the impurity, and by 25 percent on the more distant Cu. This can be understood as an effect of hole doping from  $O_i$  (see later) when  $E_F$  is approaching a van-Hove DOS peak as in other cuprates. More distant atoms of the other types (Ba, Hg, and O) have their local DOS very much like those of the undoped HBCO, i.e. only very small local DOS values. Already the second layer

from the O-stripe seems to have restored its local character as in undoped HBCO, except for the modest increase of the Cu-d DOS.

The doping is important for the high- $T_c$  in HBCO, but it is not clear if this is due to the high Cu-d DOS (and the presumed conservation of a FS cylinder, see later), or if the very large increase of the DOS close to the impurity is the essential point. The grouping of the impurities into stripes, instead of having them spread out as in the disorder case, permits to have the long-range effect on Cu-d. In fact, the local Cu-d DOS is essentially unchanged among all Cu in the striped case, it is 7 percent lower on the 3rd layer and 3.5 percent lower on the 2nd layer compared to the 1st layer from the impurity. The variation of the local Cu-d DOS in the disordered case is a bit larger, at most 20 percent (no sites go beyond the 2nd layer). From these results one may suspect that the important mechanism of O-doping is to enforce the Cu-d DOS and the generic cylindrical FS that is typical for the high  $T_c$  cuprates [52, 67], and by grouping the impurities into stripes or clusters one can avoid to have bad short-range effects from the impurity itself.

The changes in the FS from doping is studied by comparing the down-folded FS of the elementary cell into the Brillouin Zone (BZ) for the supercell. This is easier to do than the instructive method of folding supercell FS's into the BZ for the elementary cell [73]. The first step is to fold down the elementary FS of the large BZ into the smaller BZ of the corresponding supercells. The result of this procedure is shown in Fig. 3 for 3 levels of  $E_F$  corresponding to different hole doping. Fig. 4 shows the 3 FS's for the undoped, striped and disordered supercells in a plane halfway between the BZ center and the maximum of  $k_z$ . The bands are calculated in 210 k-points, and the dots in the Fig. indicate where a band energy is within a small energy window around  $E_F$ . The energy window is narrower in the high-DOS cases in order to have not too many dots. The left panel shows the FS for the undoped supercell. As expected, this FS is close to that shown in the lower left part of Fig 3. Practically all features of the FS agree. The middle panel, showing the FS of the striped supercell, can be compared with the down-folded middle panel in Fig. 3, which is labeled " $E_F - .1$ ". The FS feature  $f$  in the original FS, which show up at  $f$  in the down-folded FS without doping (lower left), has moved to  $f''$  at this hole doping. Also other pieces of FS, such as the merging of the points  $e$  and  $d$  into  $e''$  and  $d''$ , confirm the higher level of hole doping for the basic FS cylinder. This is also corroborated by the effective valence charge within the Cu spheres, which on the average decreases by  $0.04 \text{ el./Cu}$ , see Table II. The Cu closest to  $O_i$  has a larger reduction, about  $0.06 \text{ el./Cu}$ . However, on top of the FS panel for the striped supercell there is a horizontal local array of dots that cannot be seen from the down-folded simple FS. A large DOS contribution is coming from these points, and it is likely due to the O-i band. The right panel of Fig. 4 shows the FS for the disordered supercell. Here it is not easy to see resemblance with any

of the down-folded FS. The wide structure in the lower part of the panel, and the horizontal lines in the middle, have no correspondences in Fig. 3. This suggests that when the O-doping is high enough, and the O-i are spread out to allow for some electronic overlap between them, they tend to destroy much of the original cuprate FS. The effective hole doping is slightly larger than for the striped case, about 0.05 el./Cu, with the largest value still at 0.06 el./Cu for the Cu closest to  $O_i$ .

These results suggest that if the oxygen interstitials are well separated they can still provide an essential hole doping for the rest of the lattice, while the local perturbation near the interstitial ion will only have small effects on the region in between. In this case there could be that superconductivity occurs in a filamentary region which is separated from the stripes.

The calculated local DOS distributions in different regions suggest that it can be energetically favorable for the impurities to form clusters or stripes rather than to have them isolated and spread out. The (hole) charge transfer ( $\Delta Q$ ) to the interior region far from the stripes,  $\Delta Q = N_i \cdot \Delta E$  leads to a gain of kinetic energy from that region;  $\Delta E_i = \Delta Q \cdot \Delta \epsilon_i$ . The local DOS  $N_i$  is small here, which makes  $\Delta \epsilon_i$  and  $\Delta E_i$  large. Since the DOS at the stripe,  $N_s$ , is large, there will be a small loss in kinetic energy ( $\Delta E_s$ ) from this region;  $\Delta E_s = \Delta Q \cdot \Delta \epsilon_s$ , since  $\Delta \epsilon_s$  is small, and totally there is a kinetic energy gain. However, the DOS will be equally high everywhere if the distribution of O-i is uniform, and the gain and loss of kinetic energy will cancel even if there is a transfer between different regions. These arguments are just indicative, since hybridization and potential energy contributions are missing.

TABLE II: Absolute values of local moments ( $\mu_B/\text{Cu}$ ) on Cu in spin polarized calculations where magnetic fields  $\pm 0.4$  eV are applied on all Cu in an AFM pattern. The last column shows  $Q_{Cu}$ , the average number of valence electrons with the Cu MT-sphere.

	average near $O_i$		far from $O_i$	$Q_{Cu}$
undoped	0.30	-	-	10.40
striped	0.29	0.29	0.30	10.36
disordered	0.29	0.28	0.30	10.35

The large difference in the DOS between the 3 cases suggests that spin-fluctuations could appear more easily in the impurity phases. This should be the case for ferromagnetism (FM) according to the Stoner model. However, anti-ferromagnetism (AFM) is stabilized in undoped cuprates and AFM spin-fluctuations are likely in hole doped cuprate systems especially when they are coupled to phonon distortions [70, 71]. Thermal disorder can alter local magnetic moments and contribute to spin fluctuations [72, 74].

It is not certain that a high DOS will promote AFM fluctuations, and in order to compare the ability for AFM

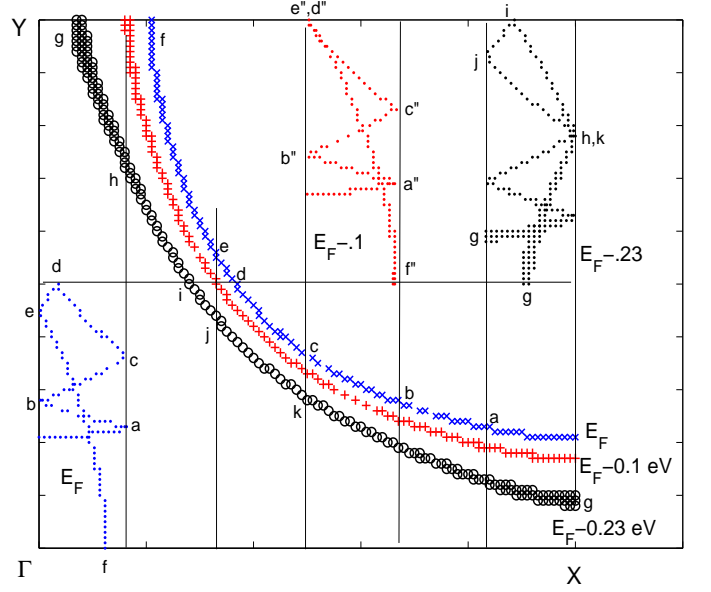


FIG. 3: (Color online) Upper large panel ( $\Gamma$ -X-Y) show the Fermi surface for one unitcell of undoped HBCO. The "x" is at the calculated  $E_F$ , the "+" for 0.1 eV down shifted, and "o" for 0.23 eV down shifted  $E_F$ . The small panels show how these FS look after folding the bands into the BZ for the 6x2 supercell.

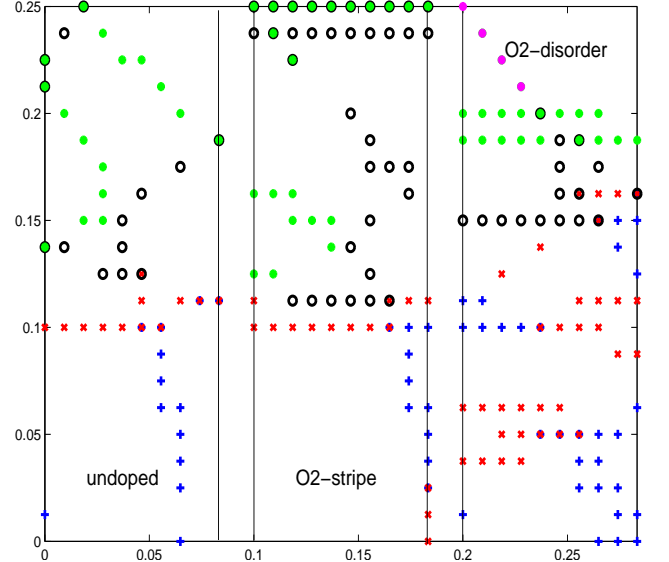


FIG. 4: (Color online) The FS of  $\text{Hg}_{12}\text{Ba}_{24}\text{Cu}_{12}\text{O}_{48+N}$  for  $N=0$  and 2 (as stripe and "disordered"). The different marks indicate different bands in the supercell band structure. It is seen that the undoped FS agree well with what is expected, i.e the folded FS shown at the bottom left of Fig. 4. The FS for the supercell with the O-stripe agree in part with the folded, downshifted (0.1 eV) FS shown in Fig. 4, and hence the doping has induced a hole doping. However, there is a new band and FS at the top that cannot be explained by from the simple folding.

spin fluctuations in the 3 cases we perform spin-polarized calculations where identical AFM fields are applied on all Cu. The results show very small differences in the AFM response between undoped, striped and disordered supercells. The reason is probably that the electronic overlap between O-i and Cu is small since they are in different layers.

The average absolute value of the local moment on Cu is highest in the undoped case, see Table II. This is consistent with the fact that real undoped cuprates are AFM insulators, while with hole doping the systems become metallic, and the stable AFM is gradually replaced by AFM fluctuations.

#### IV. CONCLUSION.

Stripes of O-i dopants in mercury based cuprates should contribute to a potential modulation with the for-

mation of a new quasi 1D band with a peak formation in the DOS at the band edge. The spatial regions far from the O-i wires and the immediate impurity clusters are spatially and electronically separated. The very high DOS within the stripes indicate that its local electronic structure is very different from the rest of the cuprate. It is tempting to view the stripe as a highly conducting "wire" within a typical cuprate which is less conducting. It is possible that high temperature superconductivity takes place in a *third* intermediate filamentary region intermediate the *first* O-i rich wires, highly doped regions, formed by clustering of O interstitials and the *second* spacial regions oxygen-poor empty of the dopant wires where spin fluctuations are expected. This scenario should be verified or discarded by space resolved angular resolved photoemission ARPES experiments, tunneling or optical spectroscopy on well defined surfaces using nanobeams.

- 
- [1] P. Littlewood, Nature Materials, **10**, 726 (2011).
  - [2] M. Fratini, N. Poccia, A. Ricci, G. Campi, M. Burghammer, G. Aeppli and A. Bianconi, Nature **466**, 841 (2010).
  - [3] N. Poccia, M. Fratini, A. Ricci, G. Campi, L. Barba, A. Vittorini-Orgeas, G. Bianconi, G. Aeppli, A. Bianconi, Nature Materials, **10**, 733 (2011).
  - [4] D. Di Castro, G. Bianconi, M. Colapietro, A. Pifferi, N. L. Saini, S. Agrestini, and A. Bianconi, The European Physical Journal B - Condensed Matter and Complex Systems **18**, 617 (2000),
  - [5] A. Bianconi, M. Lusignoli, N. L. Saini, P. Bordet, . Kvik, and P. G. Radaelli, Physical Review B **54**, 4310 (1996)
  - [6] J. A. Slezak, J. Lee, M. Wang, K. McElroy, K. Fujita, B. M. Andersen, P. J. Hirschfeld, H. Eisaki, S. Uchida, and J. C. Davis, Proceedings of the National Academy of Sciences **105**, 3203 (2008).
  - [7] B. M. Andersen, P. J. Hirschfeld, and J. A. Slezak, Physical Review B **76**, 020507 (2007).
  - [8] M. Pompa, S. Turt, A. Bianconi, F. Campanella, A. M. Flank, P. Lagarde, C. Li, I. Pettiti, and D. Udron, Physica C: Superconductivity **185-189**, 1061 (1991).
  - [9] A. Bianconi and M. Missori, in Phase separation in cuprate superconductors, edited by: E. Sigmund, K. A. Miller (Springer-Verlag, 1994).
  - [10] A. Bianconi, Solid State Communications **91**, 1 (1994).
  - [11] A. Bianconi, N. L. Saini, T. Rossetti, A. Lanzara, A. Perali, M. Missori, H. Oyanagi, H. Yamaguchi, Y. Nishihara, and D. H. Ha, Phys. Rev. B **54**, 12018 (1996).
  - [12] A. Bianconi, S. Agrestini, G. Bianconi, D. Di Castro, and N. L. Saini, Journal of Alloys and Compounds **317-318**, 537 (2001).
  - [13] F. V. Kusmartsev, D. Di Castro, G. Bianconi, and A. Bianconi, Physics Letters A **275**, 118 (2000),
  - [14] P. Barnes, M. Avdeev, J. Jorgensen, D. Hinks, H. Claus, and S. Short, Phys. Rev. B **72**, 134515 (2005).
  - [15] J. M. Hill, B. Dabrowski, J. F. Mitchell, and J. D. Jorgensen, Physical Review B **74**, 174417 (2006).
  - [16] T.H. Geballe and M. Marezio, Physica **C 469**, 680 (2009).
  - [17] W.B. Gao, Q.Q. Liu, L.X. Yang, Y. Yu, F.Y. Li, C.Q. Jin and S. Uchida, Phys. Rev. B **80**, 094523 (2009).
  - [18] O. Chmaissem, I. Grigoraviciute, H. Yamauchi, M. Karppinen, and M. Marezio, Phys. Rev. B **82**, 104507 (2010).
  - [19] M. Marezio, O. Chmaissem, C. Bougerol, M. Karppinen, H. Yamauchi, and T. H. Geballe, APL Materials **1**, 021103 (2013)
  - [20] P. Giraldo-Gallo, et al., Nature Communications **6**, 8231 (2015).
  - [21] A. Ricci, N. Poccia, G. Campi, B. Joseph, G. Arrighetti, L. Barba, M. Reynolds, M. Burghammer, H. Takeya, Y. Mizuguchi, Y. Takano, M. Colapietro, N. Saini, A. Bianconi Phys. Rev. B **84**, 060511, (2011).
  - [22] A. Ricci, N. Poccia, B. Joseph, G. Arrighetti, L. Barba, J. Plaisier, G. Campi, Y. Mizuguchi, H. Takeya, Y. Takano, et al., Superconductor Science and Technology **24**, 082002 (2011)
  - [23] A. Ricci et al. Scientific Reports **3**, 2383 (2013)
  - [24] A. Ricci, N. Poccia, G. Campi, F. Coneri, L. Barba, G. Arrighetti, M. Polentarutti, M. Burghammer, M. Sprung, M.v Zimmermann and A. Bianconi, New Journal of Physics **16**, 053030 (2014).
  - [25] G. Campi, A. Ricci, N. Poccia, L. Barba, G. Arrighetti, M. Burghammer, A. S. Caporale, and A. Bianconi, Phys. Rev. B **87**, 014517 (2013).
  - [26] G. Campi, A. Ricci, N. Poccia, A. Bianconi, Journal of Superconductivity and Novel Magnetism **27**, 987 (2014).
  - [27] I. Zeljkovic, et al. Nature Materials **11**, 585 (2012).
  - [28] I. Zeljkovic and J. E. Hoffman, Physical Chemistry Chemical Physics **15**, 13462 (2013),
  - [29] I. Zeljkovic, et al., Nano Lett. **14**, 6749 (2014).
  - [30] A. Bianconi, International Journal of Modern Physics B **14**, 3289 (2000).
  - [31] V. Kresin, Y. Ovchinnikov and S. Wolf, Physics Reports **431**, 231 (2006).
  - [32] G. Bianconi, Physical Review E **85**, 061113 (2012);
  - [33] G. Bianconi, Journal of Statistical Mechanics: Theory and Experiment **2012**, P07021 (2012).
  - [34] G. Bianconi, Europhysics Letters **101**, 26003 (2013).

- [35] K. I. Kugel, A. L. Rakhmanov, A. O. Sboyshakov, N. Poccia, and A. Bianconi, Phys. Rev. B. **78**, 165124 (2008).
- [36] K.I. Kugel, A.L. Rakhmanov, A.O. Sboyshakov, F.V. Kusmartsev, N.Poccia, and A.Bianconi, Superconductor Science and Technology **22**, 014007 (2009)
- [37] A.Bianconi, N.Poccia, A.O. Sboyshakov, A.L. Rakhmanov, and K.I. Kugel, Superconductor Science and Technology **28**, 024005 (2015)
- [38] A. Bianconi, Nature Physics **9**, 536 (2013).
- [39] M. Fratini, N. Poccia and A. Bianconi Journal of Physics: Conference Series **108**,1012036 (2008)
- [40] A. Bianconi Journal of Superconductivity **18**, 625 (2005).
- [41] A. Bianconi, Journal of Physics and Chemistry of Solids **67**, 567 (2006),
- [42] A. Bianconi, S. Agrestini, G. Campi, M. Filippi, and N. L. Saini, Current Applied Physics **5**, 254 (2005),
- [43] A. Bianconi, and T. Jarlborg Novel Superconducting Materials **1**, 37 (2015)
- [44] T.Jarlborg and A.Bianconi, Scientific Reports **6**, 24816 (2016)
- [45] A.Bianconi and T.Jarlborg, EPL (Europhysics Letters) **112**, 37001 (2015)
- [46] T. Jarlborg, Appl. Phys. Lett. **94**, 212503, (2009).
- [47] T. Jarlborg and A. Bianconi, Phys. Rev. B **87**, 054514 (2013).
- [48] T. Jarlborg, and A. Bianconi, J. Supercond. Nov. Magn. **29**, 615 (2016)
- [49] T. Jarlborg, B. Barbiellini, R.S. Markiewicz and A. Bansil, Phys. Rev. B **86**, 235111 (2012)
- [50] T. Jarlborg, A. Bianconi, B. Barbiellini, R. S. Markiewicz, and A. Bansil, J. Supercond. Nov. Magn. **26**, 2597 (2013),
- [51] T. Jarlborg, Phys. Rev. B **68**, 172501 (2003).
- [52] T. Jarlborg and G. Santi, Physica C **329**, 243 (2000).
- [53] T. Jarlborg, Phys. Rev. B **84**, 064506 (2011).
- [54] G. Campi, etal. Nature **525**, 359 (2015).
- [55] G., Campi, A. Bianconi J. Super. and Nov. Magn. **29**, 627 (2016)
- [56] Z.Wu, N.Saini, and A.Bianconi, Physical Review B **64**, 092507 (2001)
- [57] A.Lanzara, N.L. Saini, A.Bianconi, F.Duc, and P.Bordet, Physical Review B **59**, 3851 (1999)
- [58] P.Bordet, F.Duc, P.G. Radaelli, A.Lanzara, N.Saini, A.Bianconi, and E.V. Antipov, Physica C: Superconductivity **282-287**, 1081 (1997),
- [59] A. Bianconi, S.Doniach, and D.Lublin, Chemical Physics Letters **59**, 121 (1978)
- [60] J. Garcia, A. Bianconi, M. Benfatto, and C. R. Natoli, Le Journal de Physique Colloques **47** C8-49 (1986).
- [61] O.K. Andersen, Phys. Rev. B **12**, 3060 (1975).
- [62] B. Barbiellini, S.B. Dugdale and T. Jarlborg, Comput. Mater. Sci. **28**, 287 (2003).
- [63] W. Kohn and L.J. Sham, Phys. Rev. **140**, A1133 (1965)
- [64] O. Gunnarsson and B.I. Lundquist, Phys. Rev. B **13**, 4274 (1976).
- [65] B. Barbiellini and T. Jarlborg, Phys. Rev. B **50**, 3239 (1994).
- [66] T. Jarlborg, Phys. Rev. B **64**, 060507(R), (2001).
- [67] W.E. Pickett, Rev. Mod. Phys. **61**, 433 (1989).
- [68] A. Damascelli, Z.-X. Shen and Z. Hussain, Rev. Mod. Phys. **75**, 473, (2003).
- [69] B. Barbiellini, P. Genoud, J.Y. Henry, L. Hoffmann, T. Jarlborg, A.A. Manuel, S. Massidda, M. Peter, W. Sadowski, H.J. Scheel, A. Shukla, A.K. Singh and E. Walker, Phys. Rev. B **43**, 7810 (1991).
- [70] T. Jarlborg, Physica C **454**, 5, (2007).
- [71] T. Jarlborg, Phys. Rev. B **76**, 140504(R), (2007).
- [72] T. Jarlborg, J. of Supercond. and Novel Magn., **28**, 1231 (2014)
- [73] P. Lazić, D. Pelc, M. Požek, V. Despoja, and D.K. Sunko, J. of Supercond. and Novel Magn., **28**, 1299, (2014)
- [74] T. Jarlborg, Phys. Rev. B **89**, 184426 (2014).